Soluble TREM2 levels reflect the recruitment and expansion of TREM2^{+} macrophages that localize to fibrotic areas and limit NASH

Tim Hendrikx, Florentina Porsch, Máté G. Kiss, Dragana Rajcic, Nikolina-Papac Milicevic, Constanze Hoebinger[1], Laura Göderle, Anastasiya Hladik, Lisa E. Shaw, Hauke Horstmann[9], Sylvia Knapp, Sophia Derdak, Martin Bilban, Lena Heintz, Marcin Krawczyk, Rafael Paternostro, Michael Trauner, Matthias Farlik, Dennis Wolf, Christoph J. Binder

Table of contents

SUPPLEMENTARY METHODS

Animal Experiments

Ldlr$^{-/-}$ mice (stock no. 002207), CD45.1 C57/Bl6J (stock no. 002014) and *Ccr2*$^{-/-}$ (stock no. 004999) were originally acquired from The Jackson Laboratory (Bar Harbor, ME, USA). C57Bl6/J mice were acquired from our in-house breeding facility at the Medical University of Vienna, Austria. *Trem2*$^{-/-}$ mice[1] were originally provided by Marco Colonna, Washington University, St. Louis, MO, USA. *Trem2*$^{-/-}$*Ldlr*$^{-/-}$ mice were generated by crossing *Trem2*$^{-/-}$ with *Ldlr*$^{-/-}$ mice in house. All mice were on a C57Bl6/J background. Age- and sex-matched littermate controls aged 8 weeks or older were used for all experiments and co-housed to reduce potential microbiota-related confounding effects. Mice were bred under barrier-specific pathogen-free conditions at the Department of Biomedical Research or the Department of Laboratory Animal Science and Genetics of the Medical University of Vienna, Austria and housed in individually-ventilated cages with a 12-hour dark-/light-cycle with *ad libitum* access to food and water. Experiments were be performed with the minimal necessary number of mice. To estimate the sample size needed to achieve adequate power to detect differences, we used the online tool http://biomath.info/power/ttest.htm and data from comparable previous experiments. All experimental studies, interventions and sample sizes were approved by the Animal Ethics Committee of the Medical University of Vienna and the Austrian Federal Ministry of Education, Science and Research, and were performed according to Good Scientific Practice and national and international institutional guidelines (License numbers BMWF 66.009/0336-V/3b/2018; BMWF 2020-0.787.152; BMWF 66.009/0179-V/3b/2019).

Bone Marrow Transplantation

C57Bl6/J or *Ldlr*$^{-/-}$ mice received two doses of **γ**-irradiation (2x6Gy) and their bone marrow was reconstituted with 4x10^6 bone marrow cells isolated from *Trem2*$^{-/-}$ and *Trem2*$^{+/+}$ male littermates or from CD45.1$^+$ C57Bl6/J donor mice. Recipient mice subsequently recovered for 6 weeks prior to further experimental interventions to allow for reconstitution of the hematopoietic compartment.

Dietary interventions

For MCD studies, male C56Bl6/J mice received a methionine- and choline-deficient diet (MCD, U8958, SAFE Labs, Rosenberg, Germany) for up to 4 weeks. For HFC studies, *Ldlr*$^{-/-}$ and *Trem2*$^{-/-}$*Ldlr*$^{-/-}$ mice were fed a high fat-high cholesterol (HFC) diet containing 21% milk fat and 0.21% cholesterol (TD88137, Ssniff Spezialdiäten GmbH, Soest, Germany) for up to 12 weeks. For dietary switching studies, mice were switched back to standard chow after 2 weeks of HFC or MCD diet as specified in figure legends. For high-fat diet (HFD) studies, male C57Bl6/J mice received a 60% kcal fat diet (D12492, Research Diets Inc, New Brunswick, NJ, USA). In the STAM model, male C57Bl6/J mice received a low-dose subcutaneous streptozotocin injection (200 µg/mouse, Sigma, MO, USA) at two days after birth to induce diabetes, which was followed by administration of a 46% HFD (Purified Diet 235 HF, Safe diets, France) for up to 8 weeks. All diets and water were previously irradiated or autoclaved for sterility and were administered *ad libitum*.

Generation of Bone Marrow-derived Macrophages (BMDM)

To generate BMDM for subsequent gene expression analysis and conditioned media experiments, femora and tibiae of *Trem2*$^{-/-}$ and *Trem2*$^{+/+}$ littermates were flushed using

PBS supplemented with 2% heat-inactivated fetal calf serum (FCS), homogenized by gentle passage through a 21-gauge needle followed by passage through a 70µm cell strainer. Red blood cells were lysed using hemolysis buffer (Morphisto, Offenbach am Main, Germany). Cells were cultured in petri dishes at 37°C and 5%CO_2 in Dulbecco's Modified Eagle Medium (DMEM)+GlutaMax (Gibco, Thermo Fisher Scientific) supplemented with 10% heat-inactivated FCS, penicillin (100 U/ml), streptomycin (100µg/ ml) and antimycotics (Sigma-Aldrich), as well as 10% L929-conditioned medium. After 7 days, some cells were stimulated for 16 hours in full culture medium containing 20ng/ml recombinant mouse Interleukin-4 (Peprotech, Thermo Fisher Scientific). BMDMs were collected in Trizol for RNA isolation as described below.

Biochemical Analyses

Blood was collected in EDTA collection tubes (Greiner Bio-One, Germany) and plasma obtained by centrifugation at 1000xg for 20 minutes. Plasma levels of ALT were determined using Reflotron ALT strips on a Reflotron Plus (Roche). Plasma and hepatic triglyceride and cholesterol levels were measured according to manufacturer's instructions using Liquid Reagents kit (GPO-PAP Triglyceride Liquicolor kit, CHOD-PAP Cholesterol Liquicolor kit, HUMAN Biochemica and Diagnostica mbH, Wiesbaden, Germany). Hepatic collagen I alpha 1 was assessed in liver homogenates using the Human pro-collagen I alpha 1 DuoSet Elisa kit according to the manufacturer's protocol (DY6220-05, R&D Systems, Minneapolis, MN, USA). Hydroxyproline content was determined as described previously[2]. Protein content was measured using the Pierce BCA Protein Assay Kit (Thermo Fisher Scientific, Waltham, MA, USA).

Immunohistochemistry

Liver sections were embedded in OCT compound and 7 µm frozen sections were stained and quantified for Mac-1 (1/1000) for infiltrating macrophages, NIMP (1/500) for neutrophils, CD3 (1/500) for T cells, and with Oil Red O (Sigma-Aldrich, Vienna, Austria) to determine lipid content as done previously[3]. The *In Situ* Cell Death Detection Kit TMR Red TUNEL staining kit (Roche Diagnostics, Rotkreuz, Switzerland) was used according to manufacturer's instructions to assess cell death. TUNEL+ cells were quantified in at least three randomly selected pictures of liver sections per mouse. Sirius Red staining was done to detect fibrosis on frozen liver sections to process overlay with spatial imaging slides. Double staining of liver cryosections for CD63 and aSMA was done after prior citrate-based antigen retrieval (C9999, Sigma-Aldrich) followed by initial staining for α-SMA (1/200) using the Vectastain ABC-AP reagent kit (AK-5000, Vector Laboratories) and Vector Blue substrate solution (SK-5300, Vector Laboratories), followed by staining for CD63 (1/250) using the Vectastain Elite ABC kit (PK-6100, Vector Laboratories) in combination with Vector Nova Red substrate kit for peroxidase (SK-4800, Vector Laboratories), according to the manufacturer's staining procedures. Formalin-fixed tissue samples were embedded in paraffin and 4 µm sections were stained with Hematoxylin and Eosin (HE) for general morphology, Masson's Trichrome (according to the manufacturer's protocol; HT15-1KT, Sigma-Aldrich) and Sirius Red for liver fibrosis detection. At least four high-power fields of the liver per mouse were randomly selected for quantification of Sirius red positive staining using Image J Software. Masson's Trichrome staining was scored blinded for the amount of positive staining on the whole liver section. Sections were photographed using a Zeiss AxioImager A1

microscope with AxioCam MRC5 using the Zen 2.3 Pro Software (Carl Zeiss AG, Jena, Germany).

RNA Isolation

For whole liver RNA isolation, 50mg tissue pieces of left lateral liver lobes were snap frozen in liquid nitrogen. Frozen tissue in QIAzol lysis reagent was homogenized mechanically using stainless steel beads in a Tissue Lyser II (Qiagen, Hilden, Germany). RNA was extracted by QIAzol according to the manufacturer's instructions. For RNA extraction from sorted cells, RNA was extracted according to the manufacturer's instructions using an RNeasy Micro kit (Qiagen, Hilden, Germany) or using the PeqGOLD Total RNA kit (VWR International, Radnor, PA, USA). RNA content and quality were assessed using Nanodrop (Peqlab).

cDNA Generation and qPCR

For quantitative real-time PCR, up to 1µg of RNA was reverse transcribed using the High Capacity cDNA Reverse Transcription kit (Applied Biosystems, Thermo Fisher, Waltham, MA, USA) to generate cDNA. Real-time PCR was performed on a CFX96 Real-Time PCR System (Bio-Rad Laboratories, Hercules, CA, USA) using the KAPA SYBR FAST kit (Thermo Fisher, Waltham, MA, USA) and the primers indicated below. Gene expression was normalized to *18S*.

Gene (mouse)	**Forward Sequence (5'-3')**	**Reverse Sequence (3'-5')**
18S	AGTCCCTGCCCTTTGTACACA	CGATCCCAGGGCCTCACTA
Tnfa	CCCATATACCTGGGAGGAGTCTTC	CATTCCCTTCACAGAGCAATGAC
Cxcl1	GCTGGGATTCACCTCAAGAA	TCTCCGTTACTTGGGGACAC
Cxcl2	AGTGAACTGCGCTGTCAATG	TTCAGGGTCAAGGCAAACTT

Trem2	CTACCAGTGTCAGAGTCTCCGA	CCTCGAAACTCGATGACTCCTC
Gpnmb	GGCTACTTCAGAGCCACCATCA	CTTTGCAGGTCACAGTGAAGTCC
Lgals3	AACACGAAGCAGGACAATAACTGG	GCAGTAGGTGAGCATCGTTGAC
Mmp12	GCTAGAAGCAACTGGGCAAC	ACCGCTTCATCCATCTTGAC
Clec7a	AGAACCACAAGCCCACAGAA	ATCCAATTAGGAAGGCAAGG
Saa1	GGCTGCTGAGAAAATCAGTGATG	TCAGCAATGGTGTCCTCATGTC
Il1b	TGGACCTTCCAGGATGAGGACA	GTTCATCTCGGAGCCTGTAGTG
Acta2	TGCTGACAGAGGCACCACTGAA	CAGTTGTACGTCCAGAGGCATAG
Col1a1	AACCCTGCCCGCACATG	CAGACGGCTGAGTAGGGAACA
Col3a1	GACCAAAAGGTGATGCTGGACAG	CAAGACCTCGTGCTCCAGTTAG
Tgfb1	TGATACGCCTGAGTGGCTGTCT	CACAAGAGCAGTGAGCGCTGAA
Ccl2	GCTACAAGAGGATCACCAGCAG	GTCTGGACCCATTCCTTCTTGG
Itgam	ATGGACGCTGATGGCAATACC	TCCCCATTCACGTCTCCCA
Itgax	CTGGATAGCCTTTCTTCTGCTG	GCACACTGTGTCCGAACTCA
Cd36	GCCAAGCTATTGCGACATGA	AAAAGAATCTCAATGTCCGAGACTTT
Fabp4	TGAAATCACCGCAGACGACAGG	GCTTGTCACCATCTCGTTTTCTC
Fabp5	GACGACTGTGTTCTCTTGTAACC	TGTTATCGTGCTCTCCTTCCCG
Lipa	GCAAAGGTCCCAGACCAGTT	TCATCAAACTGAAGGCCCAGA
Lpl	GGGAGTTTGGCTCCAGAGTTT	TGTGTCTTCAGGGGTCCTTAG
Ctsb	AGTCAACGTGGAGGTGTCTGCT	GTAGACTCCACCTGAAACCAGG
Ctsd	TAAGACCACGGAGCCAGTGTCA	CCACAGGTTAGAGGAGCCAGTA
Gpnmb	GGCTACTTCAGAGCCACCATCA	CTTTGCAGGTCACAGTGAAGTCC
Il1a	ACGGCTGAGTTTCAGTGAGACC	CACTCTGGTAGGTGTAAGGTGC
Nlrp3	CCACAGTGTAACTTGCAGAAGC	GGTGTGTGAAGTTCTGGTTGG
Ccl5	CCTGCTGCTTTGCCTACCTCTC	ACACACTTGGCGGTTCCTTCGA
Cxcl9	TCCTTTTGGGCATCATCTTC	TTCCCCCTCTTTTGCTTTTT
Vcam1	GTGTTGAGCTCTGTGGGTTTTG	TTAATTACTGGATCTTCAGGGAATGAG
Lgals1	GTAACACCAAGGAAGATGGGACC	TCATGTCCGTCTGGCAGCTTGA
Anxa1	TGTATCCTCGGATGTTGCTGCC	CCATTCTCCTGTAAGTACGCGG

Prdx1	TGCCAAGTGATTGGCGCTTCTG	AGCAATGGTGCGCTTGGGATCT
Timp1	TCTTGGTTCCCTGGCGTACTCT	GTGAGTGTCACTCTCCAGTTTGC
Col1a2	TTCTGTGGGTCCTGCTGGGAAA	TTGTCACCTCGGATGCCTTGAG

Bulk RNA Sequencing

For RNA sequencing, RNA was quantified and its quality was assessed using the Qubit 2.0 Fluorometric Quantitation system (Life Technologies, Thermo Fisher, Waltham, MA, USA) and the Experion Automated Electrophoresis System (BioRad, Hercules, CA, USA). Libraries were subsequently sequenced at the Biomedical Sequencing Facility at the CeMM Research Center for Molecular Medicine of the Austrian Academy of Sciences using the HiSeq 3000/4000 platform (Illumina, San Diego, CA, USA) in a 25bp single-read configuration. Data were processed as previously described[3]. GO term and KEGG Pathway analyses were performed using the Enrichr platform[4].

Tissue Collection and Generation of Single Cell Suspensions

For sorting and single cell RNA seq experiments, livers were collected and rinsed in ice-cold PBS prior to dissociation. Tissue was subsequently digested using the Mouse Liver Dissociation kit according to manufacturer's instructions using the GentleMacs Tissue Dissociator (both Miltenyi Biotech, Bergisch Gladbach, Germany). For flow cytometric analysis, livers were dissociated mechanically and digested for 20 minutes at 37°C using 450 U/ml collagenase I (LifeTech Austria, Vienna, Austria), 125 U/ml collagenase XI (Sigma-Aldrich, Vienna, Austria), 60 U/ml DNase I (LifeTech Austria, Vienna, Austria) and 60 U/ml hyaluronidase (Sigma-Aldrich, Vienna, Austria) in PBS followed by red blood cell lysis (Morphisto, Offenbach am Main, Germany). Samples were passed through 100 µm strainers prior to staining.

Flow Cytometry and Cell Sorting

For flow cytometry, blocking and staining were performed in PBS supplemented with 2% heat-inactivated FBS at 4°C in the dark. For blocking of Fc receptor interactions, $1x10^6$ cells were incubated with 2.5 µg/ml of unconjugated anti-CD16/CD32 antibody (clone 93, eBioscience, Invitrogen). After washing, cells were incubated with the following antibodies for 30 minutes: anti-Ly6C Brilliant Violet605 or FITC (clone HK1.4; BioLegend, San Diego, CA, USA, anti-F4/80 PerCP/Cyanine 5.5 (clone BM8; BioLegend), anti-CD45 FITC or APC (clone 30-F11; BioLegend), anti-Ly6G PE-Cy7 (clone 1A8; BD Biosciences) or PE (clone 1A8; BioLegend), anti-CD11b Alexa Fluor 700 or APC (clone M1/70; eBioscience), anti-CLEC4F Alexa Fluor 647 (clone 3E3F9; BioLegend), anti-VSIG4 PE-Cy7 (clone NLA14; eBioscience) and anti-TIM4 PE (clone 54(RMT4-54); eBioscience). For some experiments, cells were subsequently stained according to manufacturer's instructions using 7AAD and AnnexinV (eBIosciences) to assess cell viability. After staining, all samples were immediately acquired on a BD LSRII Fortessa (BD Biosciences) and subsequently analysed using FlowJo Software V10 (FlowJo Inc, BD Life Sciences). For sorting of macrophage and monocyte populations, single cell suspensions were stained in ice-cold PBS supplemented with 0.5% BSA and 2 mM EDTA using the same antibody panels as for flow cytometry, followed by cell viability staining using 7-AAD (eBioscience). Cells were flow-sorted at 4°C on a FACS Aria II cytometer (BD Biosciences, NJ, USA) using a 100 µm nozzle and immediately processed for downstream applications.

Single Cell RNA Sequencing

Single cell suspensions were processed as described in the dark in ice-cold PBS supplemented with 0.05% BSA. Cells were blocked using anti-CD16/32, followed by

staining for CD45-APC (clone 30-F11, BioLegend) and viability staining using 7-AAD. Live 7-AAD- CD45+ cells were flow-sorted at 4°C on a FACS Aria II cytometer (BD Biosciences, NJ, USA) using a 100 µm nozzle. CD45+ cells from 4 mice per group were pooled in equal proportions and immediately processed according to manufacturer's instructions by encapsulation into single cell gel beads (GEMs) and unique molecular identifier (UMI) barcoding using the Chromium Next GEM 5' v2 chemistry Single Cell kit (10x Genomics, Pleasanton, CA, USA). Libraries were sequenced on a NovaSeq 6000 (Illumina, San Diego, CA, USA) using paired-end 2x50bp setting as following recommendations by 10X Genomics. Sequencing data were processed using the Cell Ranger Single Cell software suite[5]. Raw sequencing reads were analysed with the Bioconductor analysis package SEURAT[6]. Doublets were removed from *Trem2*$^{+/+}$ and *Trem2*$^{-/-}$ raw data sets using the R package DoubletFinder[7]. Only cells with a count of unique genes between 200 and 4000 and a fraction of mitochondrial genes < 0.05 were included for further analysis. In the combined data set of *Trem2*$^{+/+}$ and *Trem2*$^{-/-}$, 1483 unique genes and 4202 total gene transcripts were detected in a total of 10,589 cells. Individual data sets from *Trem2*$^{+/+}$ and *Trem2*$^{-/-}$ donors were merged with the SEURAT v3 VST-integration workflow[6]. Samples were pre-processed and cleaned of unwanted cellular events to contain a minimum of 200 unique genes/cell. For all subsequent analyses, UMAP embedding and Louvain clustering were employed at a resolution of 0.8 and 30 PCA dimensions. Gene expression was displayed as violin plots on normalized RNA counts for each cell type defined by Louvain-clustering. Differentially expressed genes were determined on normalized RNA-counts only within genes expressed in a minimum of 25% of cells in one of the tested groups and a minimum fold change between two tested groups of 0.25. Only adjusted p-values < 0.05 (Bonferroni) were considered

significant. Gene module enrichment was performed according to Tirosh et al[8] on normalized RNA-counts. Input gene lists were retrieved from reported DE-genes in the study by Ramachandran et al[9]. Enrichment of module scores per cell were overlaid color-coded on UMAP plots. Cell types were annotated based on differentially expressed genes across all clusters and automated annotation to published gene signatures with SingleR[10]. Filtered transcriptomes from leukocyte clusters identified as macrophage clusters served as alternative input for data integration and analysis (macrophage reclustering).

Spatial Transcriptomics

Visium Spatial Transcriptomics (ST) experiments were performed at the Genomics and the Imaging Core Facilities of the Medical University of Vienna following the current protocols published on the 10x Genomics webpages (CG000160_DemonstratedProtocol_MethanolFixationandHEStaining_RevC.pdf and CG000239_VisiumSpatialGeneExpression_UserGuide_RevD.pdf). Since a RIN of > 7.0 is required for this protocol, RNA quality was assessed on snap-frozen liver tissue cryo-sections before undertaken a full ST protocol using a Bioanalyzer 2100 RNA pico assay (Agilent). Additionally, a tissue optimization experiment (CG000238_VisiumSpatialTissueOptimizationUserGuide_Rev_A.pdf) was performed with imaging the fluorescence footprint testing of 6 different timepoints of tissue permeabilization on an IX83 Live Imaging Microscope (Olympus) and visual inspection of the image identified 20 minutes as optimal permeabilization time, which was then used on the spatial gene expression slides. A total of six sections from livers collected from six *Ldlr*$^{-/-}$ mice (3 chow- and 3 HFC-fed for 2 weeks) were used. Sections were cut in a pre-cooled cryostat at 10µm thickness onto four 6.5mm x 6.5mm capture areas

with 4992 oligo-barcoded spots. Each spot covers a 55µm area with a 100µm center-to-center distance, which should be expected to encompass 6-10 liver cells. Slides then underwent fixation and HE staining with immediate imaging on IX83 Live Imaging Microscope (Olympus) at 10x magnification. Tissue underwent permeabilization with proprietary enzyme (20 minutes), reverse transcription and second strand synthesis were performed on the slide with cDNA quantification by qRT-PCR using KAPA SYBR FAST-qPCR kit (KAPA Biosystems) and analyzed on the CFX96 Touch Real-Time PCR Detection Systems (BioRad). qRT-PCR results (Cq value at 25% of peak fluorescence) informed cDNA amplification. Following library construction as per manufacturer's instructions ST libraries were QC-checked for correct insert size on a Bioanalyzer 2100 (Agilent) using a High Sensitivity DNA kit and quantified using the KAPA-Illumina PCR quantification kit (KAPA Biosystems). Libraries were pooled at 4nM concentration with a sample ratio corresponding to the surface area of tissue coverage obtained from the H&E imaging. Pooled libraries were loaded at a concentration of 1.8 pM and sequenced on six NextSeq500 flowcells (High output, v 2.5, Illumina) to a total depth of 59,000-88,000 reads per tissue covered spot (mean achieved: 71,891 reads) which corresponds to the amount of reads per spot recommended in the 10x Genomics protocol. Raw sequencing data were demultiplexed and processed with Spaceranger version 1.3.1. The quality of the reads was assessed using FASTQC[11]. As an additional control of the tissue permeabilization and mRNA capture process and to identify potential leakage of transcripts from the tissue, the UMI density in areas of the capture areas that were not covered by tissue was inspected using a .json mask file for Spaceranger that identified all spots of the capture area as tissue; no leakage was detected. Reads were mapped against the GRCm38 mouse reference genome, and Gencode version M23 (Ensembl 98)

transcripts were quantified. This generated a dataset of 14400 tissue-covered spots with a median of 3455 genes detected per spot (see table below with more details). Spaceranger output data were imported into R for use with Seurat version 4.0.5 [12]. A Seurat object was created for each capture area using the Read10X and the CreateSeuratObject functions. In Seurat, samples were merged using the Seurat::merge function, and merged data were normalized and scaled using the NormalizeData function with the LogNormalize method, the FindVariableFeatures function with the vst methods and the ScaleData function for scaling and centering of the data. In addition, data were batch-corrected with Harmony[13] following a workflow suggested by 10x Genomics for Visium (https://www.10xgenomics.com/resources/analysis-guides/correcting-batch-effects-in-visium-data) using the slide membership of each sample as covariate. The first two dimensions of a UMAP reduction were plotted (Figure S6A). In addition, bulk RNA alignment was performed aligning for each sample all reads against the murine reference genome mm10[14] using STAR aligner[15] version 2.6.1a in 2-pass mode, disregarding the spot barcodes and UMIs. Raw reads per gene were counted by STAR, then variance-stabilizing transformed using DESeq2[16], and a principal component analysis was run using the prcomp function from the stats package. In parallel, Spaceranger output data (cloupe.cloupe file) were further analyzed in Loupe Browser 6.0.0. for cluster definition and data export. For spot composition analysis and cluster definition, captured spots were considered positive for a gene of interest when the expression of the feature was >0, while a detection of ≤0 within a spot was considered negative for the respective feature. For cluster definition using multiple marker genes, a spot was considered positive upon expression (>0) of the combination of all genes of interest, while a spot was considered negative when no

expression was detected (≤0) for any of the genes of interest. Defining direct neighbouring spots was done via manual selection in Loupe Browser 6.0.0. using the selection tools. Within each liver slide, to explore and characterize identified clusters, differentially expressed gene analysis within clustered spots was done in Loupe Browser 6.0.0. showing 'All Features' using the 'Locally Distinguishing' function to compare significant features. GO term and pathway analysis was done using the MSigDB Browser platform in the GSEA software S[17, 18]. Gene module analysis was done by importing indicated public gene sets (see supplementary table below) into Loupe Browser 6.0.0. and assessing the combined 'Feature Average' within defined clusters in each liver slide.

Sample	# spots under tissue	Mean reads/ spot	Median genes/ spot	Total genes detected	Median UMI counts/ spot	Sequenc-ing saturation
Chow 1	1.583	82.261	3.989	17.202	19.653	53.8%
Chow 2	2.615	65.541	2.974	17.390	10.733	73.3%
Chow 3	2.574	59.662	3.008	17.265	11.657	68.7%
Hfc 1	2.015	72.101	4.109	17.752	20.179	53.9%
Hfc 2	2.271	61.379	3.706	18.214	14.714	64.3%
Hfc 3	3.342	63.184	2.944	18.006	9.223	73.8%

Peritoneal Macrophage Isolation and *in vitro* Foam Cell Formation Assay

For *in vitro* foam cell formation assays, peritoneal macrophages were harvested from *Trem2*$^{+/+}$ or *Trem2*$^{-/-}$ littermates that were injected intraperitoneally with 50µl thioglycollate (Thermo Fisher Scientific, Difo Laboratories, Waltham, MA, USA) per gram bodyweight 72 hours prior. Thioglycollate-elicited macrophages were plated in RPMI-1640 medium supplemented with 10% heat-inactivated FCS and allowed to

adhere for 4 hours. Cells were subsequently treated with 10-50µg/ml of Cu-OxLDL or 50µg/ml native LDL for 24 hours. Cells were subsequently rinsed in serum-free PBS and incubated with 2µM BODIPY 493/503 (4,4-Difluoro-1,3,5,7,8-Pentamethyl-4-Bora-3a,4a-Diaza-*s*-Indacene; Invitrogen, Thermo Fisher Scientific) in PBS for 15 minutes in the dark at 37°C. Cells were washed with PBS, single cell suspensions were generated by gentle scraping and stained for flow cytometry as described above. Lipid content is assessed by comparing mean fluorescence intensity (MFI) for BODIPY-493/503 of macrophages (F4/80+CD11b+).

In vitro Fibrosis Assay

The murine fibroblast cell line NIH/3T3 were a kind gift from Prof. Erwin F. Wagner and Dr. Latifa Bakiri of the Medical University Vienna, Austria. The *in vitro* fibrosis assay using conditioned media (CM) from *Trem2*$^{+/+}$ and *Trem2*$^{-/-}$-derived BMDM was performed as previously described[19]. Briefly, to collect conditioned medium from primary BMDMs isolated from *Trem2*$^{+/+}$ and *Trem2*$^{-/-}$ littermates treated with or without IL-4 (as described above), cells were rinsed in PBS and fresh DMEM medium supplemented with 10% FCS was added. After 48 hours, medium was collected, centrifuged at 2000xg for 10 minutes, aliquoted and stored at -80°C for use.

NIH/3T3 were plated in 24-well plates at 0.6 x 10^5 cells/well at in DMEM GlutaMax supplemented with 10% heat-inactivated FCS, penicillin (100 U/ml), streptomycin (100µg/ ml) and antimycotics (Sigma-Aldrich). After 12 hours, plates were rinsed in PBS and conditioned media was added, while full DMEM or full DMEM with 5ng/ml TGF-β1 (Peprotech, Thermo Fisher Scientific) were added as controls. After 24 hours, cells were harvested for RNA analysis in Trizol as described.

Murine Soluble TREM2 ELISA

96-well MaxiSorp Nunc-Immunoplates (Invitrogen, Thermo Fisher) were coated with unconjugated TREM2 antibody (MAB17291, clone 237920, R&D Systems, Minneapolis, MN, USA) diluted 1:1000 in carbonate buffer (0.05M, pH 9.6) at 4°C overnight. After washing in PBS, plates were blocked using 1% BSA + 0.05% Tween-20 in PBS at room temperature for 4 hours. Plates were washed five times using washing buffer (0.05% Tween-20 in PBS), followed by incubated with samples diluted 1:5 in assay buffer (0.2% BSA + 0.05% Tween-20) at 4°C overnight. After washing with wash buffer five times, plates were incubated with biotinylated anti-mouse TREM2 antibody (BAF1729, polyclonal, R&D Systems) diluted 1:3000 in assay buffer at room temperature for 2 hours. Plates were then incubated with Streptavidin-HRP (R&D Systems) diluted 1:40 in assay buffer at room temperature for 1 hour in the dark after washing 5 times in wash buffer. After five final washing steps in wash buffer, plates were developed by addition of TMB substrate (Reagent A&B, R&D Systems) followed by Stop solution (2N sulfuric acid, R&D Systems) and absorbance was read at 450 nm with 570nm wavelength correction on a Synergy 2 plate reader (BioTek Instruments, Winooski, VT, USA).

Human Soluble TREM2 ELISA

Human soluble TREM2 was measured using a human sTREM2 ELISA kit (DY1828, R&D Systems) according to manufacturer's instructions. Briefly, 96-well plates were coated in mouse anti-human TREM2 capture antibody at 2 µg/ml at room temperature overnight, followed by blocking in 1%BSA-PBS at room temperature for 2 hours. Samples were diluted 1:10 in Reagent Diluent (0.1%BSA + 0.05% Tween-20 in TBS, pH 7.4, R&D Systems) and recombinant sTREM2 was used as a standard at 3000 –

46.86 pg/ml. Samples were incubated at room temperature for 2 hours, followed by incubation with biotinylated goat anti-human TREM2 detection antibody at 75ng/ml at room temperature for 2 hours. Finally, samples were incubated with streptavidin-HRP at a 1:40 dilution for 20 minutes at room temperature in the dark, followed by developing with TMB substrate for 20 minutes and Stop solution. Absorbance was read at 450 nm with 570nm wavelength correction on a Synergy 2 plate reader (BioTek Instruments, Winooski, VT, USA).

Biopsy-proven NAFLD Cohort

Patients were recruited from the Department of Internal Medicine III, Division of Gastroenterology and Hepatology, Medical University of Vienna, Austria. The study protocol was approved by the Institutional Review Boards of the Medical University of Vienna (EK 747/2011) and the local ethics committees of the participating centers and performed in accordance with the current version of the Helsinki Declaration. All patients signed an informed consent form prior to study inclusion. Hepatic ultrasonography and liver biopsy was performed on all participants. Liver biopsies of patients were reviewed in a blinded manner by two independent pathologists. FIB-4 score was calculated based on clinically available parameters as previously described (FIB-4 = age ([yr] x AST [U/L]) / ((PLT [10(9)/L]) x (ALT [U/L])(1/2))) [20]. Participants with other forms of chronic liver disease or with a history of daily alcohol intake were excluded by screening.

Saarland University Hospital Cohort

The patients (age range 19 - 86 years) were prospectively recruited from diabetes and liver outpatient clinic at Saarland University Hospital (Homburg, Germany). All patients

signed an informed consent form prior to study inclusion. Individuals with acute or chronic liver diseases, other than NAFLD, were excluded from the study. Those with other preliminary conditions (i.e. chronic kidney disease, heart failure, neurodegenerative diseases, preexisting depression, immobility) were also excluded. Fatty liver disease was assessed non-invasively by controlled attenuated parameter (CAP) and liver stiffness measurement (LSM) by Fibroscan. Patients were stratified using CAP ≥ 248 dB/m², LSM ≥ 9.12 kPa³ and LSM ≥ 13.1 kPa³ as cut-offs for significant steatosis, fibrosis and cirrhosis, respectively. The interquartile ratio of at least 20 single measurements for both values must not exceed 30%. Patients with LSM classified as fibrosis and cirrhosis were grouped in the ”fibrotic NASH” group in the figures. Laboratory blood analyses including transaminases were performed with standard clinical chemistry methods at Saarland University Central Laboratory. FIB-4 score was calculated as described above. Overall, 72.5% of the patients had diabetes mellitus type 2.

Statistical Analysis

Data comparing two groups were assessed as appropriate by two-tailed unpaired Student’s t-test or Mann-Whitney U test following evaluation of Gaussian distribution. Comparison of multiple datasets was done using one-way analysis of variance (ANOVA) with Tukey’s post-hoc test or Bonferroni correction. Statistical analyses were performed using GraphPad Prism v9.1.2. Results are expressed as mean ± standard error (SEM) unless stated otherwise. A $p \leq 0.05$ was considered statistically significant.

Data availability

The data generated in this study are available via the NCBI GEO database (accession number GSE207138) and from corresponding authors, TH and CJB, upon reasonable request.

SUPPLEMENTARY FIGURES

Supplementary Figure 1

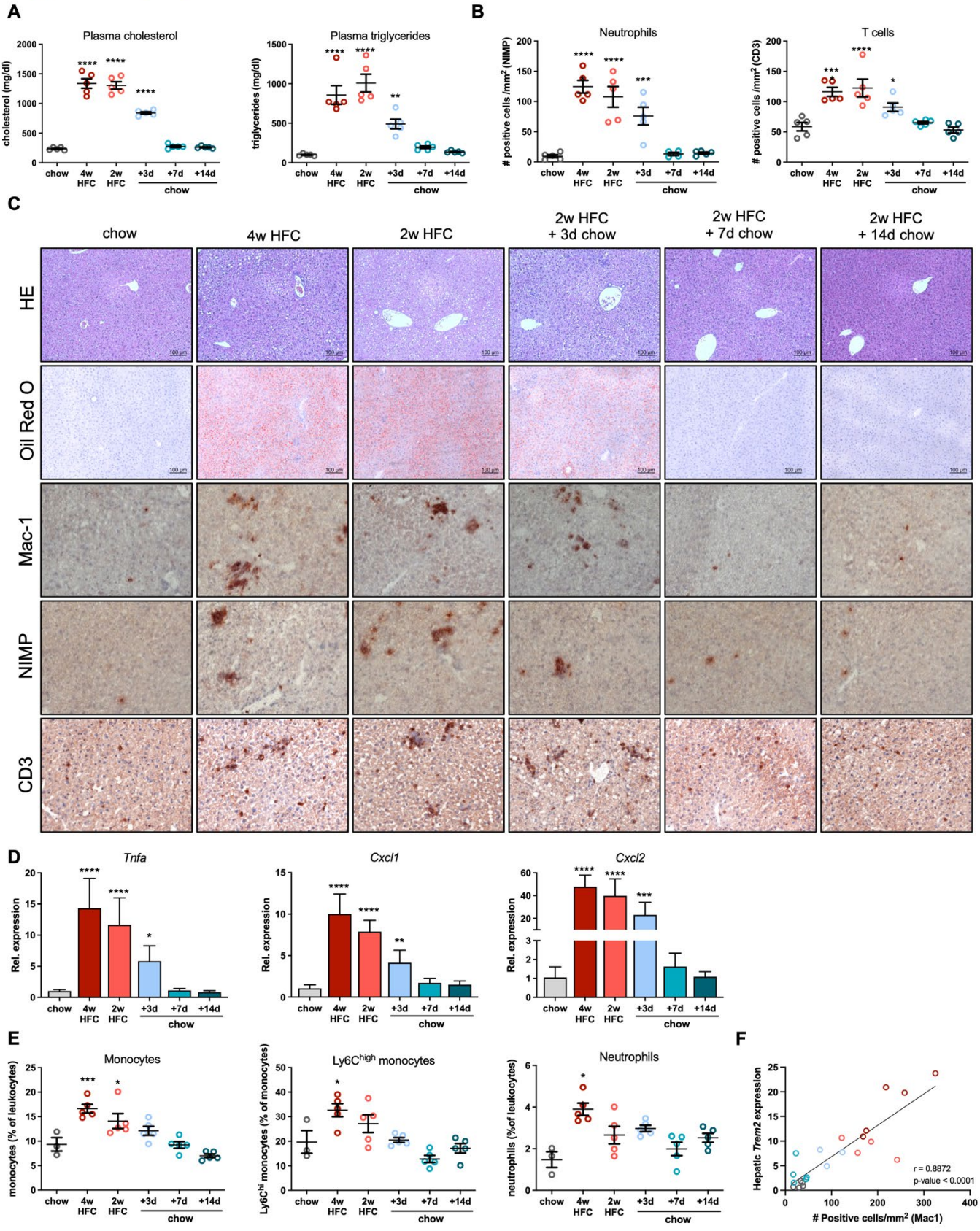

Figure S1. Characteristics of HFC diet-induced steatohepatitis in *Ldlr*$^{-/-}$ mice.

A) Systemic plasma cholesterol and triglyceride levels following dietary intervention as shown in Figure 1A.

B) Neutrophil and T cell content in the liver as assessed by immunohistochemical staining of liver sections using NIMP and CD3 antibodies, respectively.

C) Representative images showing immunohistochemical staining of liver sections by H&E, Oil Red O and for macrophages (Mac-1), neutrophils (NIMP) and T cells (CD3) (magnification 20x).

D) Gene expression of inflammatory markers *Tnfa, Cxcl1, Cxcl2* in whole liver tissue, assessed by qPCR and normalized to *18S*, shown relative to chow.

E) Frequencies of circulating total monocytes ($CD11b^+Ly6G^-$), $Ly6C^{high}$ monocytes ($CD11b^+Ly6G^-Ly6C^{high}$), and neutrophils ($CD11b^+Ly6G^+$), as quantified by flow cytometry.

F) Correlation between hepatic *Trem2* expression and liver-infiltrating macrophages ($Mac\text{-}1^+$, assessed by immunohistochemistry) in *Ldlr*$^{-/-}$ mice following dietary intervention as shown in Figure 1A.

For Figures A, B, D and E, measurements are compared to chow group. Data shown as mean ± SEM of n=4-5 mice per group. Significance is indicated compared to the respective chow group after applying one-way ANOVA with Bonferroni correction for comparing multiple groups. * indicates $p \leq 0.01$, ** $p \leq 0.01$, *** $p \leq 0.001$, **** $p \leq 0.0001$.

Supplementary Figure 2

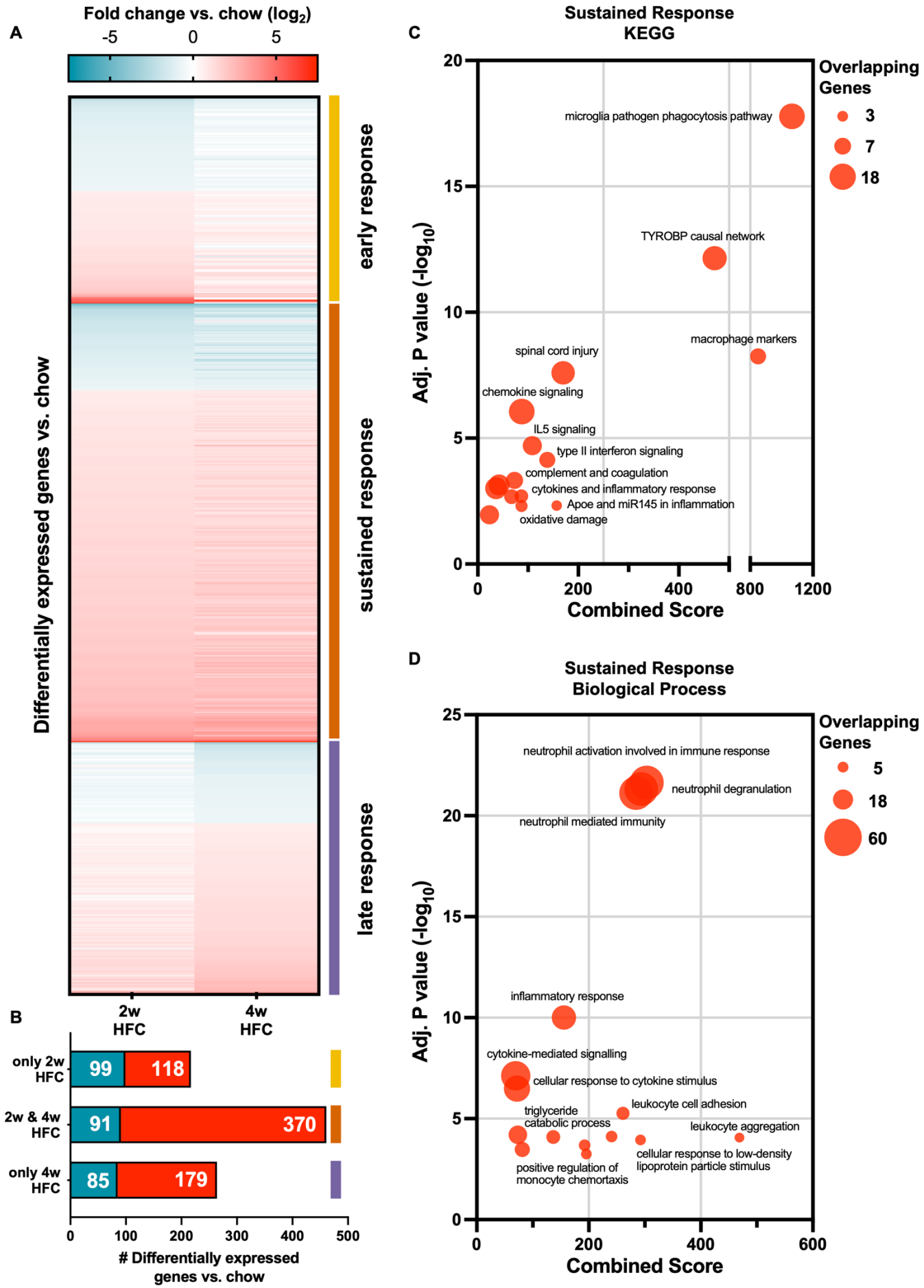

Figure S2. Hepatic gene expression profile after HFC diet in *Ldlr*$^{-/-}$ mice.

A) Gene expression changes in the livers of mice fed a HFC diet for 2 or 4 weeks compared to chow reveals genes only changed after 2 weeks HFC ('early response'), changed during both 2 and 4 weeks HFC ('sustained response') and genes changed only after 4 weeks HFC ('late response').

B) Number of genes downregulated (shown in blue) and upregulated (shown in red) compared to chow in the different diet response groups.

C) Kyoto Encyclopedia of Genes and Genomes (KEGG) pathway analysis of 'sustained response' genes.

D) Gene Ontology Biological Process analysis of 'sustained response' genes.

Supplementary Figure 3

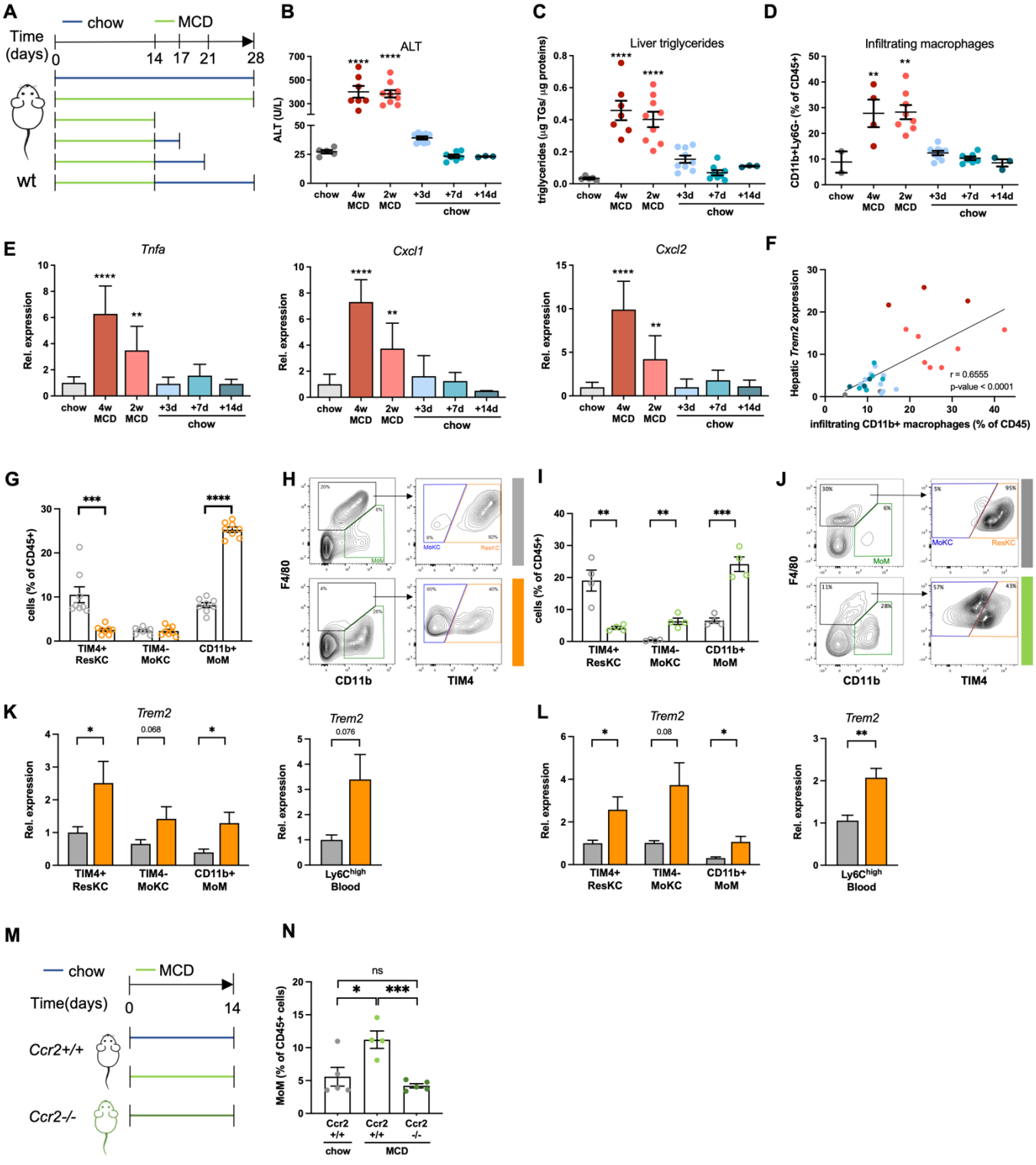

Figure S3. Characteristics of MCD diet-induced steatohepatitis.

A) Study layout. Male C57Bl6/J mice were placed on chow or a MCD diet for 2 or 4 weeks. Separate groups of mice were switched back to chow for 3, 7 and 14 days after 2 weeks of MCD diet.

B) Plasma ALT levels.

C) Liver triglyceride levels following dietary intervention, normalized to total proteins.

D) Frequency of infiltrating MoMs ($CD45^+Ly6G^-CD11b^+F4/80^-$) in the liver as assessed by flow cytometry.

E) Gene expression of inflammatory markers *Tnfa*, *Cxcl1* and *Cxcl2* in whole liver tissue, assessed by qPCR and normalized to *18S*. Data are shown relative to chow-fed mice.

F) Correlation between hepatic *Trem2* expression as assessed by qPCR (Figure 1G) and liver-infiltrating macrophages ($CD45^+Ly6G^-CD11b^+F4/80^-$, as assessed by flow cytometry) in MCD-fed C57Bl6/J mice following dietary intervention as shown in Supplementary Figure 3A.

G) Frequencies of ResKC ($Ly6G^-F4/80^+TIM4^+$), MoKC ($Ly6G^-F4/80^+TIM4^-$) and MoM ($Ly6G^-CD11b^+F4/80^-$) in the livers of chow or 10-week HFC-fed *Ldlr*$^{-/-}$ mice, assessed by flow cytometry.

H) Representative images showing gating strategy for sorting of MoM ($CD45^+Ly6G^-CD11b^+F4/80^-$, green), ResKC ($CD45^+Ly6G^-F4/80^+TIM4^+$, orange) and MoKC ($CD45^+Ly6G^-F4/80^+TIM4^-$, blue) from the livers of chow- (top) or HFC-fed (bottom) *Ldlr*$^{-/-}$ mice.

I) Frequencies of ResKC ($Ly6G^-F4/80^+TIM4^+$), MoKC ($Ly6G^-F4/80^+TIM4^-$) and MoM ($Ly6G^-CD11b^+F4/80^-$) in the livers of chow or 4 weeks MCD-fed mice, assessed by flow cytometry.

J) Representative images showing gating strategy for sorting of MoM ($CD45^+Ly6G^-CD11b^+F4/80^-$, green), ResKC ($CD45^+Ly6G^-F4/80^+TIM4^+$, orange) and MoKC ($CD45^+Ly6G^-F4/80^+TIM4^-$, blue) from the livers of chow- (top) or MCD-fed (bottom) C57Bl6/J mice.

K) Expression of *Trem2* in hepatic $TIM4^+$ ResKC, $TIM4^-$ MoKC and $CD11b^+$ MoMs sorted from the livers (left) and in $Ly6C^{high}$ monocytes sorted from the blood (right) of $Ldlr^{-/-}$ mice fed a chow (grey) or HFC (orange) diet for 4 weeks. Data are shown relative to expression in ResKC from chow-fed animals after normalization to *18S*.

L) Expression of *Trem2* in hepatic $TIM4^+$ ResKC, $TIM4^-$ MoKC and $CD11b^+$ MoMs sorted from the livers (left) and in $Ly6C^{high}$ monocytes sorted from the blood (right) of $Ldlr^{-/-}$ mice fed a chow (grey) or HFC (orange) diet for 10 weeks. Data are shown relative to expression in ResKC from chow-fed animals after normalization to 18S.

M) Experimental design of the study using $Ccr2^{-/-}$ and $Ccr2^{+/+}$ mice. Related to Figure 1L.

N) Frequency of infiltrating MoMs ($CD45^+Ly6G^-CD11b^+F4/80^-$) in the livers of mice from the study shown in Supplementary Figure 3M as assessed by flow cytometry. For B-E, measurements are compared to chow group.

Data shown as mean ± SEM of n=3-9 mice per group. Significance is indicated compared to the respective chow group after applying one-way ANOVA with Bonferroni correction or two-tailed unpaired Student's t-test for comparing multiple or two groups respectively, after testing for normality. * indicates $p \leq 0.05$, ** $p \leq 0.01$, *** $p \leq 0.001$, **** $p \leq 0.0001$.

Supplementary Figure 4

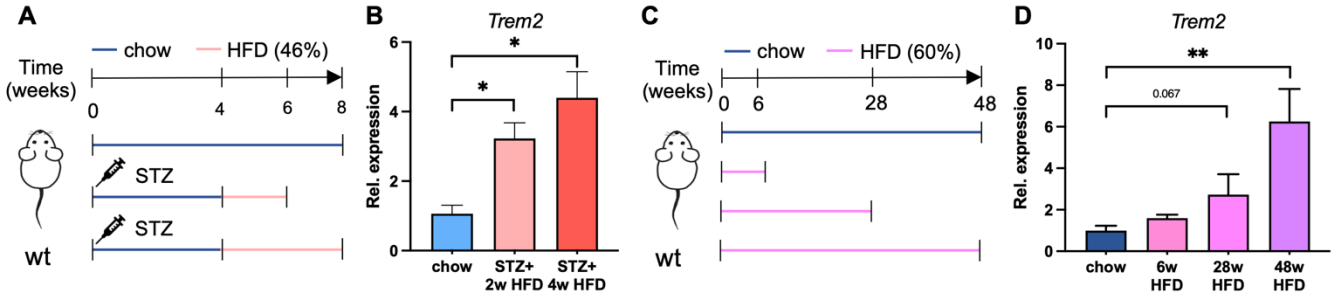

Figure S4. Hepatic *Trem2* expression in various murine NAFLD models.

A) Experimental design of STAM-induced NASH model. Male C57Bl6/J receive a single injection of low-dose streptozotocin (STZ) perinatally, followed by a 46% HFD for 2 or 4 weeks to induce steatosis or NASH, respectively.

B) Induction of *Trem2* expression in the livers of mice of the STAM model as assessed by qPCR, normalized to *18S*.

C) Experimental design of the HFD feeding study. Male C57Bl6/J mice are fed a 60% HFD for 6, 28 or 48 weeks to induce NAFLD.

D) Induction of *Trem2* expression in the livers of mice fed a HFD as assessed by qPCR, normalized to *18S*.

For B and D, significance to respective chow-fed mice is indicated after applying one-way ANOVA with Bonferroni correction for comparing multiple groups. Data shown as mean ± SEM of n=3-13 mice per group. * indicates $p \leq 0.05$, ** indicates $p \leq 0.01$,.

Supplementary Figure 5

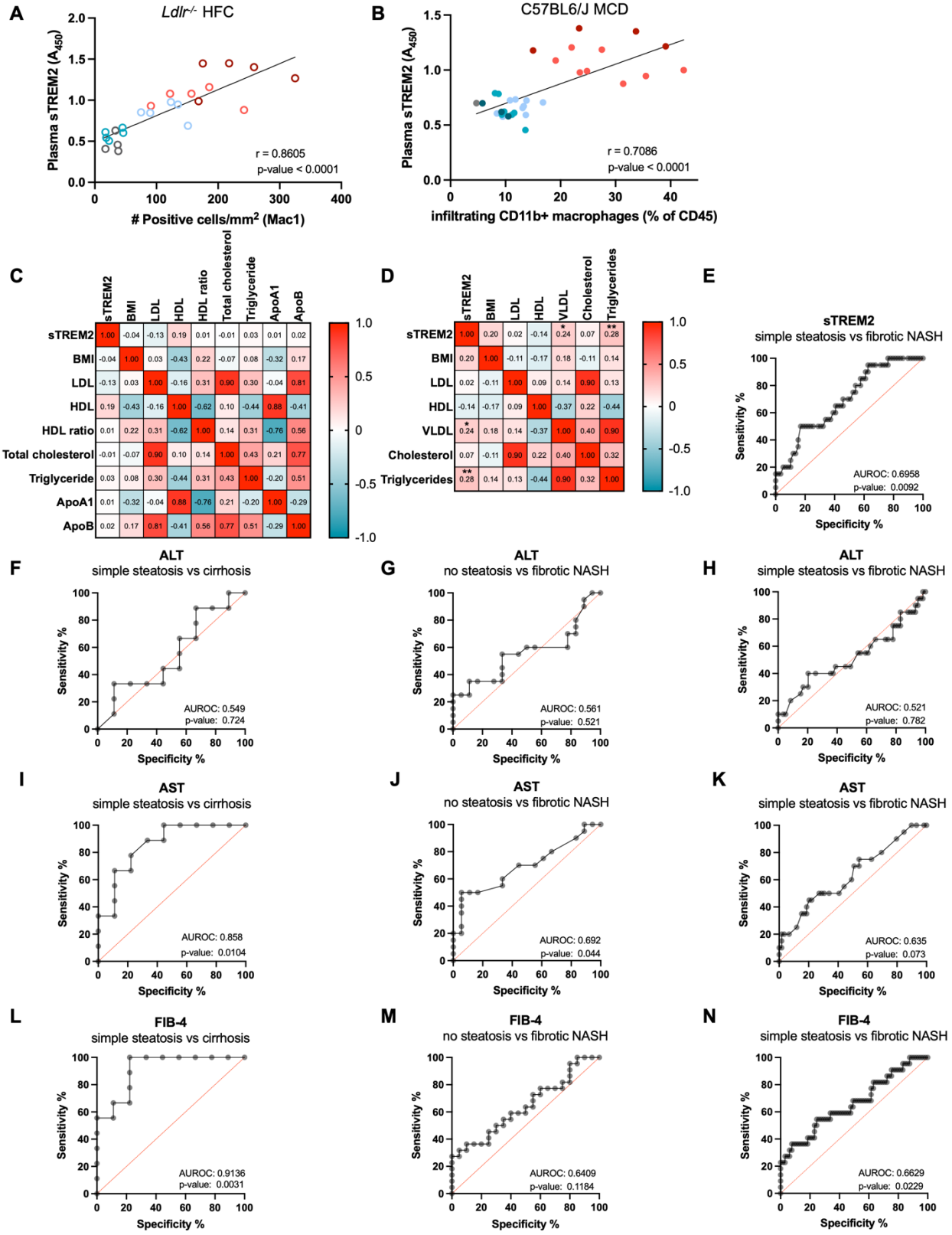

Figure S5. Plasma sTREM2 and metabolic parameters in human NAFLD cohorts.

A) Correlation of systemic sTREM2 levels and numbers of hepatic infiltrating macrophages (Mac-1$^+$, assessed by immunohistochemistry) in *Ldlr*$^{-/-}$ mice following dietary intervention as shown in Figure 1A.

B) Correlation of systemic sTREM2 levels and numbers of hepatic infiltrating macrophages (CD11b$^+$Ly6G$^-$F4/80$^-$, assessed by flow cytometry) in mice following dietary intervention as shown in Figure S3A.

C) Pearson correlation of plasma sTREM2 levels with body mass index (BMI), low-density lipoprotein (LDL), high-density lipoprotein (HDL), HDL ratio, total cholesterol, triglycerides, ApoA1 and ApoB in the biopsy-proven NAFLD cohort.

D) Pearson correlation of plasma sTREM2 levels with BMI, LDL, HDL, very-low density lipoprotein (VLDL), cholesterol, triglycerides in the cohort of patients who underwent Fibroscan measurements.

E) AUROC analysis of plasma sTREM2 levels in subjects classified as 'simple steatosis' (n=59) and 'fibrotic NASH' (n=20) in the cohort that underwent Fibroscan measurement.

F-H) AUROC analysis of serum ALT levels in patients with F) simple steatosis (n=14) or cirrhosis (n=13) in the biopsy-proven cohort and in subjects with G) no steatosis (n=18) or fibrotic NASH (n=20) and H) simple steatosis (n=59) or fibrotic NASH (n=20) in the cohort that underwent Fibroscan measurements.

I-K) AUROC analysis of serum AST levels in patients with I) simple steatosis (n=14) or cirrhosis (n=13) in the biopsy-proven cohort and in subjects with J) no steatosis

(n=18) or fibrotic NASH (n=20) and K) simple steatosis (n=59) or fibrotic NASH (n=20) in the cohort that underwent Fibroscan measurements.

L-N) AUROC analysis of FIB-4 score in patients with L) simple steatosis (n=9) or cirrhosis (n=9) in the biopsy-proven cohort and in subjects with M) no steatosis (n=20 or fibrotic NASH (n=22) and N) simple steatosis (n=59) or fibrotic NASH (n=20) in the cohort that underwent Fibroscan measurements.

* indicates $p \leq 0.05$, ** $p \leq 0.01$.

Supplementary Figure 6

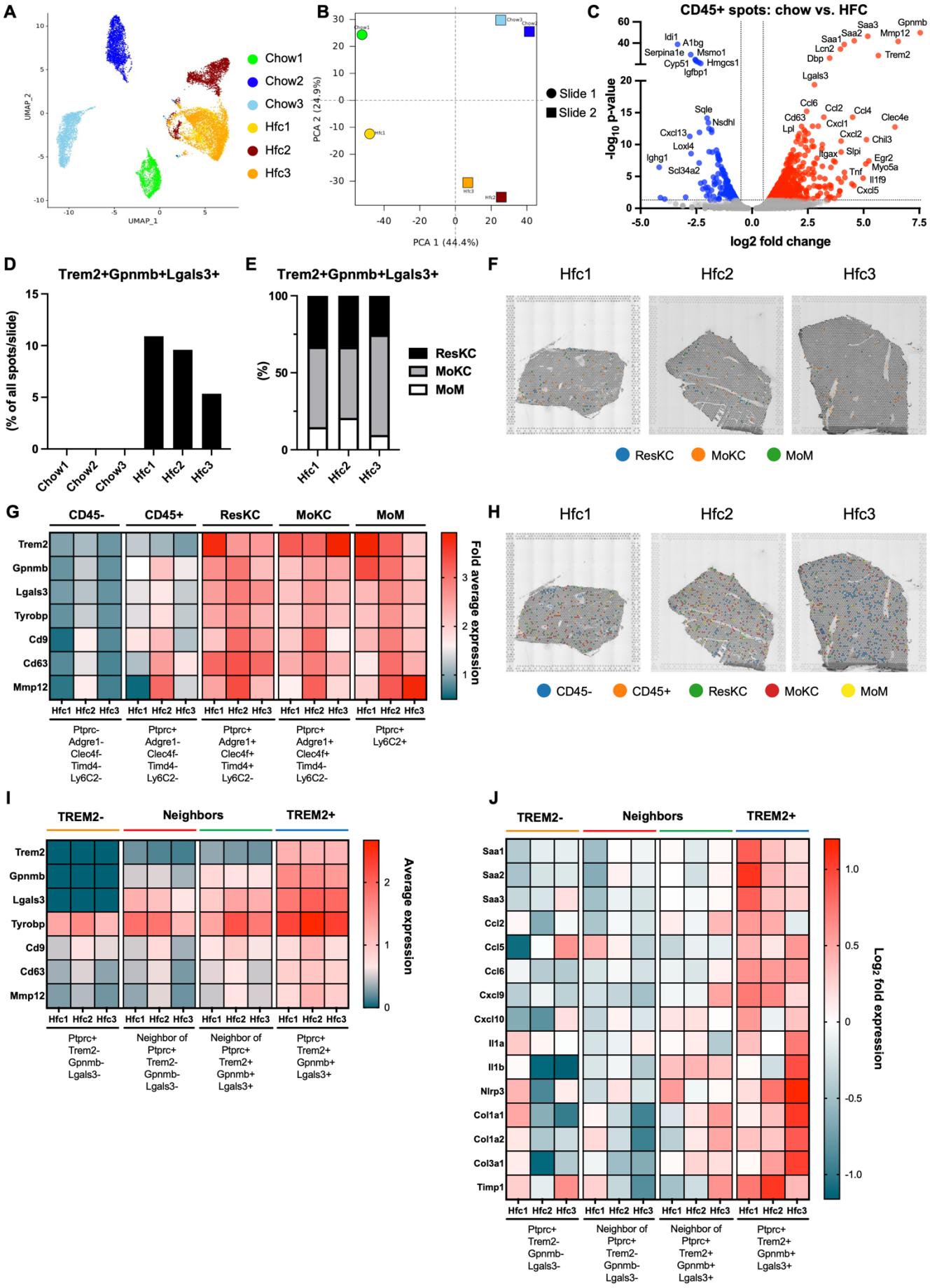

Figure S6. Spatial transcriptomics analysis of livers of chow- and HFC-fed *Ldlr*$^{-/-}$ mice.

A) Uniform Manifold Approximation and Projection (UMAP) plot of transcriptome spots from the spatial transcriptomic assessment of the livers of female *Ldlr*$^{-/-}$ mice fed a chow (Chow1, green; Chow2, dark blue; Chow3, light blue) or HFC diet (Hfc1, yellow; Hfc2, brown; Hfc3, orange) for 2 weeks.

B) Plot showing the proportions of variance for the first two components of a principal component analysis showing the biological replicates from the livers of the three chow-fed and three HFC-fed mice as shown in Supplementary Figure 6A. Circles indicate livers measured on the first slide, squares indicate livers measured on the second slide.

C) Volcano plot showing significantly up- (red) and down-regulated (blue) genes in CD45^{+} (*Ptprc*$^{+}$) spots in liver sections of HFC-fed *Ldlr*$^{-/-}$ mice compared to those of chow-fed controls, as assessed by spatial transcriptomics. A negative $\log_2$ fold change indicates downregulation in HFC group (blue), positive $\log_2$ fold change indicates upregulation in HFC group (red) relative to chow-fed mice. Non-significantly differentially expressed genes ($p>0.05$) or with a $\log_2$ fold change between -1 and 1 are shown in grey.

D) Percentage of all spots that are positive for combined detection of *Trem2*, *Gpnmb* and *Lgals3* in the indicated spatial slides.

E) Percentage of *Trem2*$^{+}$*Gpnmb*$^{+}$*Lgals3*$^{+}$ macrophage spots positive for markers of ResKC (*Adgre1*$^{+}$*Clec4f*$^{+}$*Timd4*$^{+}$), MoKC (*Adgre1*$^{+}$*Clec4f*$^{+}$*Timd4*$^{-}$) and MoM (*Ly6c2*$^{+}$) in the livers of HFC-fed mice.

F) Hfc1-3 slides showing *Trem2*$^{+}$*Gpnmb*$^{+}$*Lgals3*$^{+}$ spots positive for markers of ResKC (blue), MoKC (orange) and MoM (green) as indicated in Supplementary Figure 6E.

G) Expression of indicated genes in CD45$^-$ spots (*Ptprc$^-$Adgre1$^-$Clec4f$^-$Timd4$^-$Ly6c2$^-$*), CD45$^+$ spots (*Ptprc$^+$Adgre1$^-$Clec4f$^-$Timd4$^-$Ly6c2$^-$*), ResKC spots (*Ptprc$^+$Adgre1$^+$Clec4f$^+$Timd4$^+$Ly6c2$^-$*), MoKC spots (*Ptprc$^+$Adgre1$^+$Clec4f$^+$Timd4$^-$Ly6c2$^-$*), and MoM spots (*Ptprc$^+$Ly6c2$^+$*). Color gradient indicates $\log_2$ fold difference in gene expression.

H) Hfc1-3 slides showing spots containing markers for CD45$^-$ cells (blue), CD45$^+$ cells (orange), ResKC (green), MoKC (red) and MoM (yellow) as indicated in Supplementary Figure 6G.

I) Spatial transcriptomic assessment of expression of TREM2$^+$ macrophage-related genes in TREM2$^+$ (*Trem2$^+$Gpnmb$^+$Lgals3$^+$Ptprc$^+$*) and TREM2$^-$ (*Trem2$^-$Gpnmb$^-$Lgals3$^-$Ptprc$^+$*) spots and their neighbors as defined in Figure 3F, shown as average expression within each slide.

J) Spatial transcriptomic assessment of expression of selected genes related to the pathways shown in Figure 3E in TREM2$^+$ (*Trem2$^+$Gpnmb$^+$Lgals3$^+$Ptprc$^+$*) and TREM2$^-$ (*Trem2$^-$Gpnmb$^-$Lgals3$^-$Ptprc$^+$*) spots and their neighbors as defined in Figure 3F. Color gradient indicates $\log_2$ fold difference in gene expression within each slide.

Supplementary Figure 7

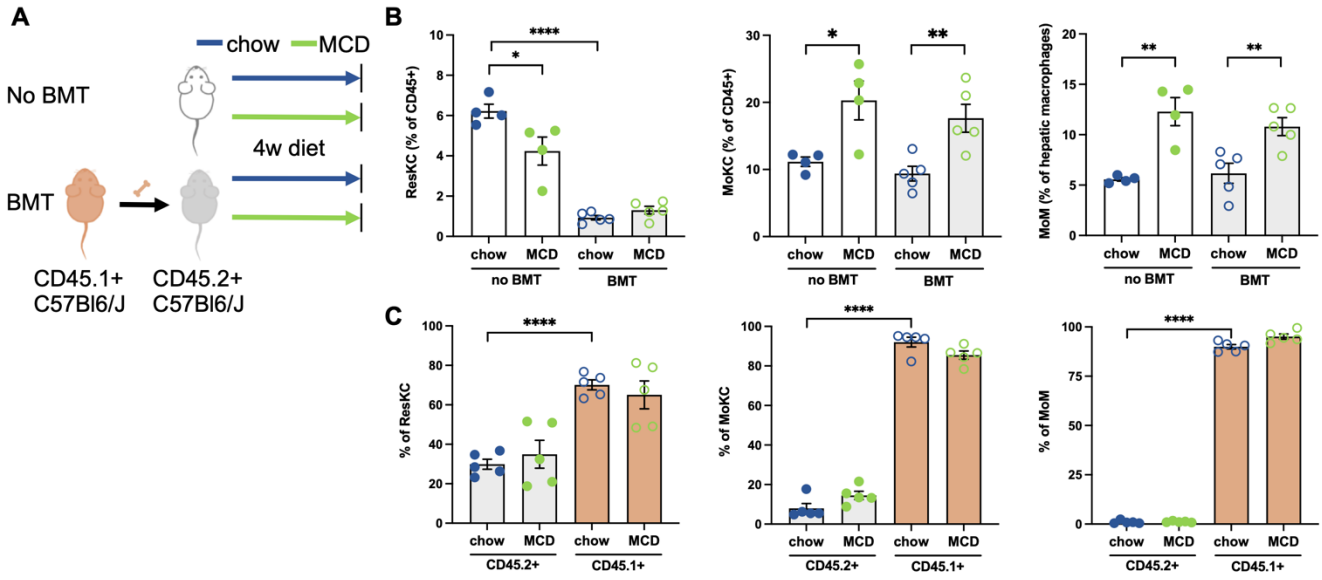

Figure S7. Hepatic Macrophage Dynamics following bone marrow transplantation with and without MCD-induced NASH.

A) Experimental design. Control C57Bl6/J females were put on a chow or MCD diet for 4 weeks. In parallel, recipient C57Bl6/J ($CD45.2^+$) females were irradiated and transplanted with bone marrow (BMT) from $CD45.1^+$ C57Bl6/J female donors to allow distinction of recipient- and bone marrow-derived cells. Following 6 weeks recovery, mice were placed on chow or MCD diet for 4 weeks and sacrificed/analysed together with non-BMT mice.

B) Percentage of ResKC ($CD45.1/.2^+Ly6G^-F4/80^+TIM4^+$, left), MoKC ($CD45.1/.2^+Ly6G^-F4/80^+TIM4^-$, middle) and MoM ($CD45.1/2^+Ly6G^-CD11b^+F4/80^-$, right) of $CD45^+$ cells in the livers of mice on chow (blue symbols) or MCD diet (green symbols) that underwent no BMT (white bars) or BMT (grey bars). Cell proportions were assessed by flow cytometry using a similar gating strategy as shown in Supplementary Figure 3J.

C) Percentage of $CD45.2^+$ (recipient mouse-derived, grey bars) and $CD45.1^+$ (donor bone marrow-derived, orange bars) cells within ResKC ($CD45.1/.2^+Ly6G^-F4/80^+TIM4^+$, left), MoKC ($CD45.1/.2^+Ly6G^-F4/80^+TIM4^-$, middle) and MoM ($CD45.1/2^+Ly6G^-CD11b^+F4/80^-$, right) in the livers of mice on chow (blue symbols) or MCD diet (green symbols).

Two-tailed unpaired Student's t-test was used to compare individual groups after testing for normality. * indicates $p \leq 0.05$, ** $p \leq 0.01$, *** $p \leq 0.001$, **** $p \leq 0.0001$.

Supplementary Figure 8

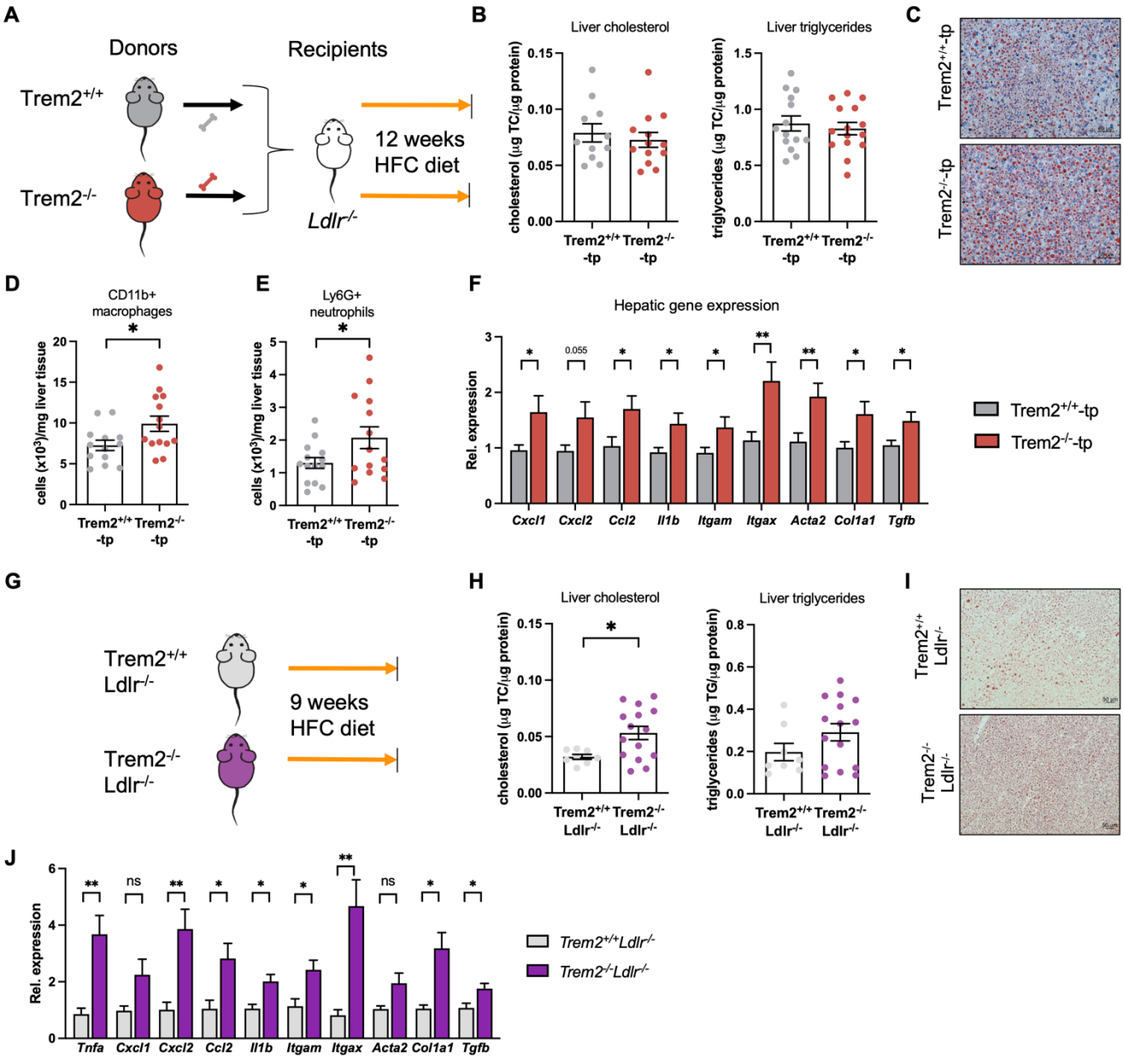

Figure S8. Hematopoietic and global TREM2 deficiency exacerbates HFC-induced NAFLD.

A) Experimental design. Male *Ldlr*$^{-/-}$ recipients were lethally irradiated and received bone marrow from *Trem2*$^{+/+}$ (Trem2$^{+/+}$-tp, grey) and *Trem2*$^{-/-}$ (Trem2$^{-/-}$-tp, red) littermates. After 6 week recovery, mice were placed on HFC diet for 12 weeks.

B) Hepatic cholesterol content and hepatic triglyceride content normalized to liver protein content.

C) Representative pictures of Oil Red O staining of liver sections (20x magnification).

D) Number of total infiltrating MoMs (CD45^{+}Ly6G^{-}F4/80^{-}CD11b^{+}) as assessed by flow cytometry.

E) Number of total neutrophils (CD45^{+}CD11b^{+}Ly6G^{+}) as assessed by flow cytometry.

F) Relative expression of *Cxcl1, Cxcl2*, *Ccl2, Il1b, Itgam, Itgax, Acta2, Col1a1* and *Tgfb*, assessed by qPCR and normalized to *18S*. Data are shown relative to Trem2$^{+/+}$-tp mice.

G) Experimental design. Male *Trem2*$^{+/+}$*Ldlr*$^{-/-}$ (light grey) and *Trem2*$^{-/-}$*Ldlr*$^{-/-}$ (purple) were placed on HFC diet for 9 weeks.

H) Hepatic cholesterol content (left) and hepatic triglyceride content (right), normalized to liver protein content.

I) Representative pictures of Oil Red O staining of liver sections (20x magnification).

J) Relative expression of *Tnfa, Cxcl1, Cxcl2, Ccl2, Il1b, Itgam, Itgax, Acta2, Col1a1* and *Tgfb,* assessed by qPCR and normalized to *18S*. Data are shown relative to *Trem2*$^{+/+}$*Ldlr*$^{-/-}$ mice.

Data shown as mean ± SEM of n=14-15 mice per group for A-F and n=9-15 mice per group for G-J. Significance is indicated after applying two-tailed unpaired

Student’s t-test for comparing two groups, after testing for normality. * indicates $p \leq 0.05$, ** $p \leq 0.01$.

Supplementary Figure 9

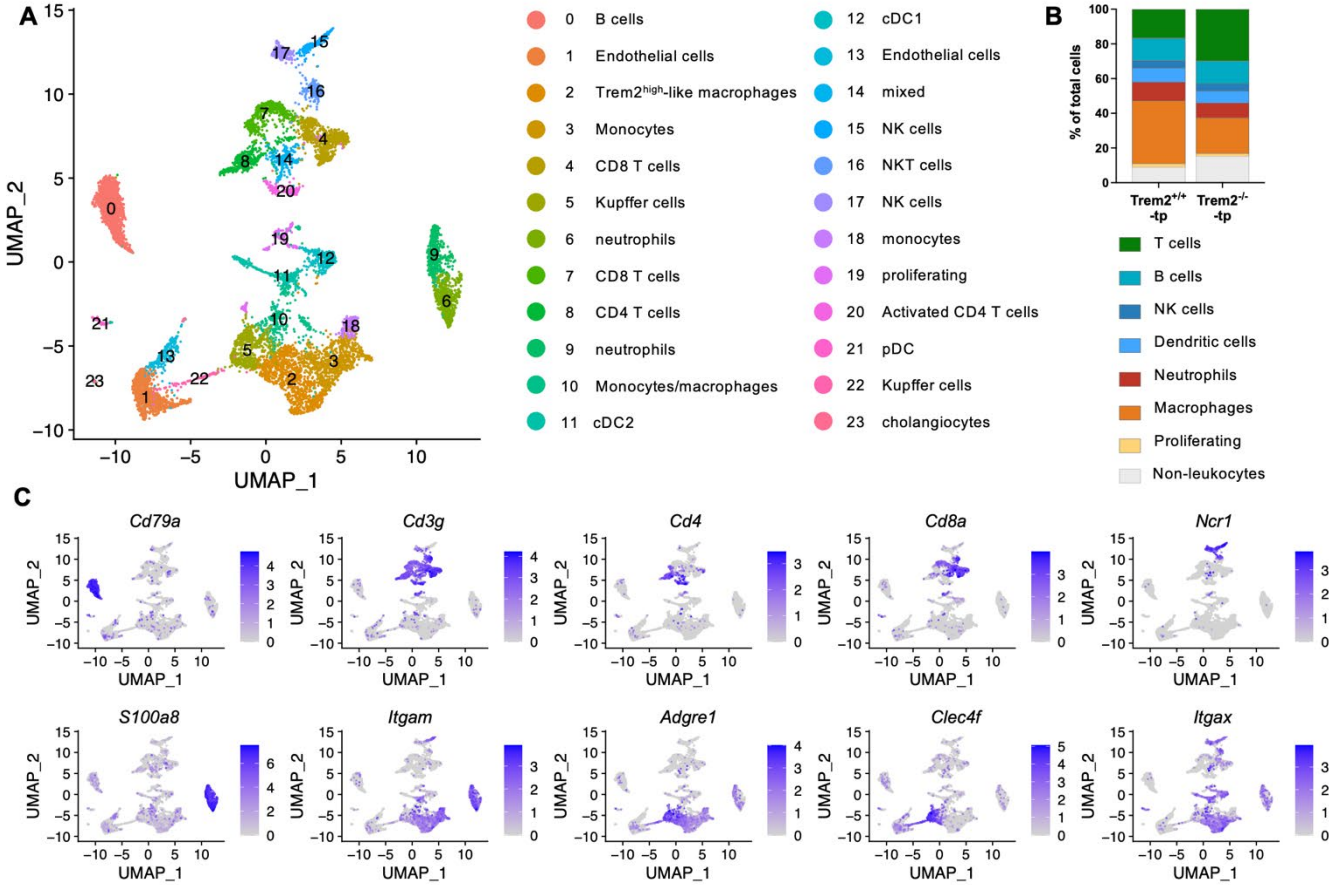

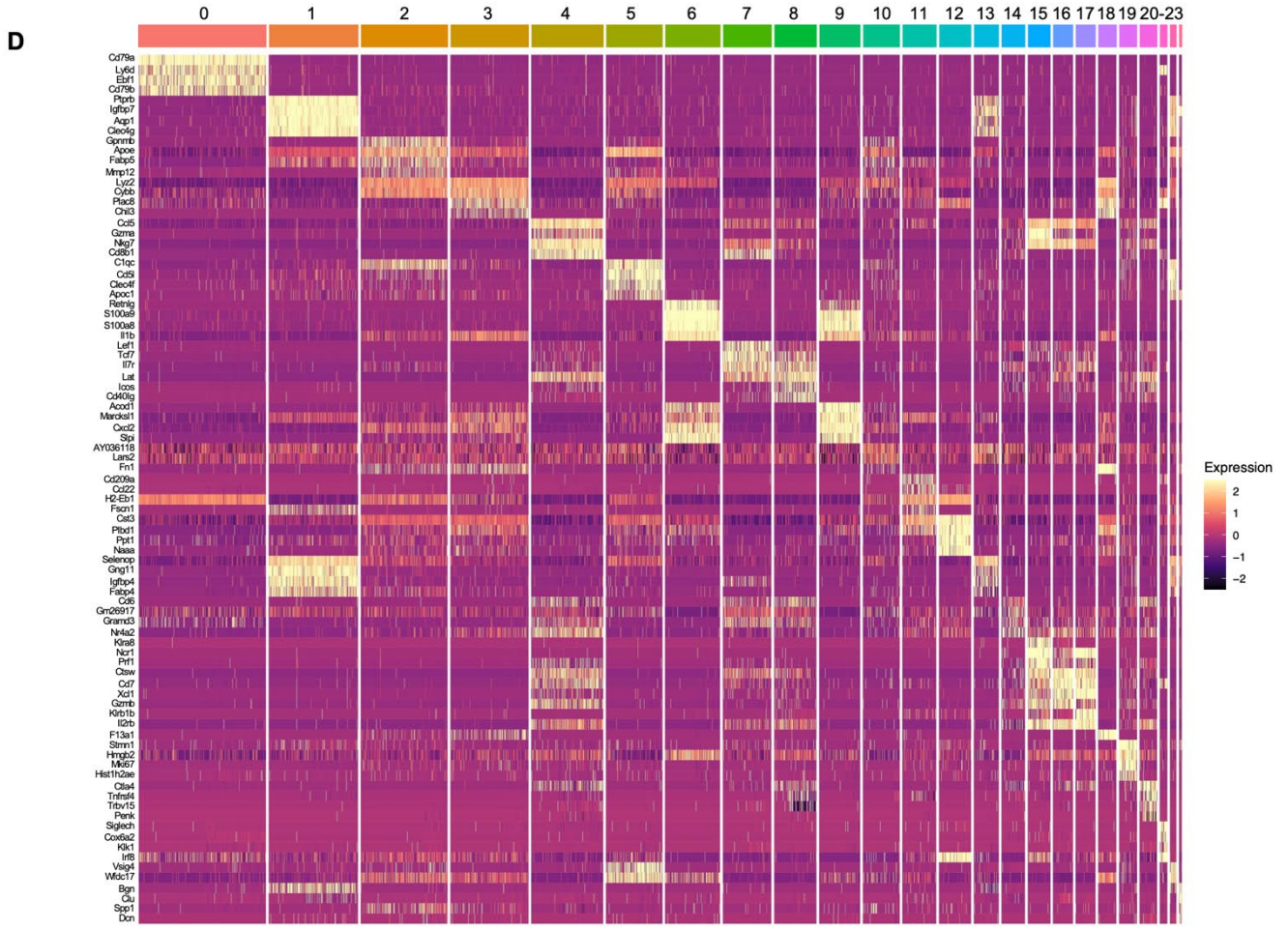

Figure S9. Hematopoietic TREM2 deficiency modulates the hepatic immune cell landscape during MCD-induced fibrotic NASH.

A) Uniform manifold approximation and projection (UMAP) showing 24 distinct clusters resulting from single cell RNA sequencing of sorted live $CD45^+$ cells from the livers of mice transplanted with *Trem2*$^{+/+}$ or littermate *Trem2*$^{-/-}$ bone marrow that were fed a MCD diet for 4 weeks (as shown in Figure 4A). Livers were pooled at equal proportion from 4 mice per group.

B) Proportion of major cell types based on clustering in Figure S9A.

C) Feature plots showing expression of key lineage-defining genes *Cd79a* (B cells) *Cd3g, Cd4, Cd8a* (T cells), *Ncr1* (NK cells), *S100a8* (neutrophils), *Itgam* (myeloid cells), *Adgre1* (macrophages), *Clec4f* (Kupffer cells), *Itgax* (dendritic cells and some macrophages) projected onto UMAP.

D) Heatmap showing top differentially expressed genes (DEGs) between clusters.

Supplementary Figure 10

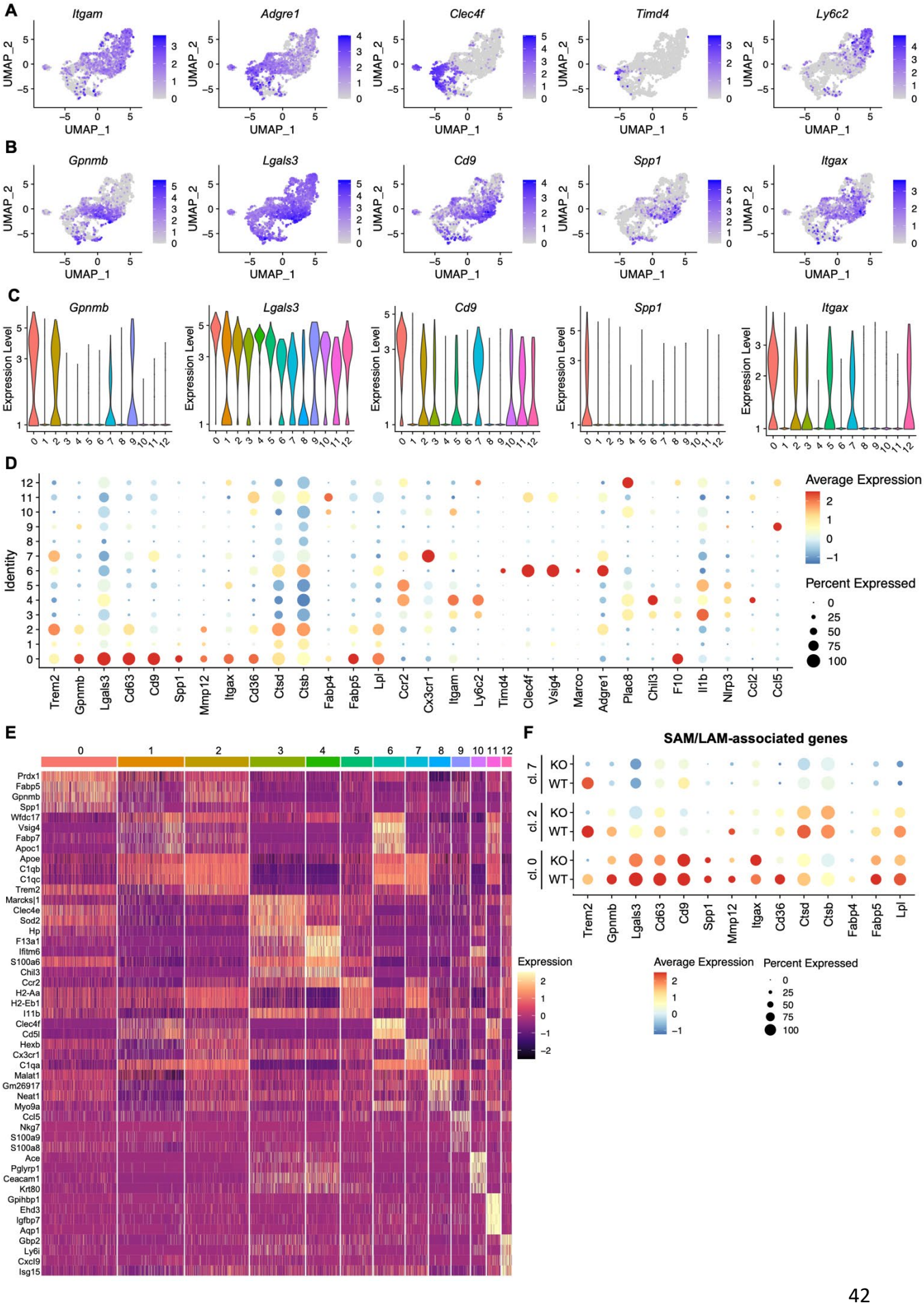

Figure S10. Hematopoietic TREM2 deficiency modulates the hepatic macrophage and monocyte landscape during MCD-induced fibrotic NASH.

A) Feature plots showing the expression of myeloid lineage-defining genes *Itgam* (monocyte and MoM), *Adgre1* (macrophage and KC), *Clec4f* (KC), *Timd4* (ResKC) and *Ly6c2* (monocyte) projected onto the UMAP of the monocyte and macrophage subclustering as shown in Figure 5A.

B) Feature plot showing the expression of the TREM2^{+} macrophage-related genes *Gpnmb, Lgals3, Cd9, Spp1* and *Itgax* projected onto the UMAP.

C) Violin plot indicating the expression of *Gpnmb, Lgals3, Cd9, Spp1* and *Itgax* across different clusters.

D) Dot plot indicating the expression of selected genes for each cluster in the *Trem2*$^{+/+}$-tp dataset only. Expression level is indicated by color (red highest expression, blue lowest expression; $\log_2$ scale where 0 is global average). Dot diameter represents the percentage of cells in the respective cluster expressing the corresponding gene.

E) Heatmap showing the top differentially expressed genes per cluster from the macrophage-monocyte subclustering.

F) Dot plot indicating the expression of selected SAM/LAM-associated genes in the TREM2+ macrophage-like clusters 0, 2 and 7 separated by genotype (WT indicates *Trem2*$^{+/+}$-tp, KO indicates *Trem2*$^{-/-}$-tp). Average $\log_2$ expression level per cluster is indicated by color, percentage of cells per cluster expressing the corresponding gene is indicated by dot size.

G) Doughnut plots showing the proportion of different clusters in the *Trem2*$^{+/+}$- (left) and *Trem2*$^{-/-}$-bone marrow chimeric mice (right). Percentages reflect proportion of

total cells per group in myeloid reclustering. Proportions are ordered by cluster number and by color coding as seen in Figure 5A.

Supplementary References

*Author names in bold designate shared co-first authorship.

[1] Turnbull IR, Gilfillan S, Cella M, Aoshi T, Miller M, Piccio L, et al. Cutting edge: TREM-2 attenuates macrophage activation. J Immunol 2006;177:3520-3524.

[2] Fuchs CD, Paumgartner G, Wahlström A, Schwabl P, Reiberger T, Leditznig N, et al. Metabolic preconditioning protects BSEP/ABCB11(-/-) mice against cholestatic liver injury. J Hepatol 2017;66:95-101.

[3] **Busch CJ, Hendrikx T,** Weismann D, Jackel S, Walenbergh SM, Rendeiro AF, et al. Malondialdehyde epitopes are sterile mediators of hepatic inflammation in hypercholesterolemic mice. Hepatology 2017;65:1181-1195.

[4] Chen EY, Tan CM, Kou Y, Duan Q, Wang Z, Meirelles GV, et al. Enrichr: interactive and collaborative HTML5 gene list enrichment analysis tool. BMC Bioinformatics 2013;14:128.

[5] Zheng GX, Terry JM, Belgrader P, Ryvkin P, Bent ZW, Wilson R, et al. Massively parallel digital transcriptional profiling of single cells. Nat Commun 2017;8:14049.

[6] **Stuart T, Butler A,** Hoffman P, Hafemeister C, Papalexi E, Mauck WM, 3rd, et al. Comprehensive Integration of Single-Cell Data. Cell 2019;177:1888-1902.e1821.

[7] McGinnis CS, Murrow LM, Gartner ZJ. DoubletFinder: Doublet Detection in Single-Cell RNA Sequencing Data Using Artificial Nearest Neighbors. Cell Syst 2019;8:329-337.e324.

[8] **Tirosh I, Izar B,** Prakadan SM, Wadsworth MH, 2nd, Treacy D, Trombetta JJ, et al. Dissecting the multicellular ecosystem of metastatic melanoma by single-cell RNA-seq. Science 2016;352:189-196.

[9] Ramachandran P, Dobie R, Wilson-Kanamori JR, Dora EF, Henderson BEP, Luu NT, et al. Resolving the fibrotic niche of human liver cirrhosis at single-cell level. Nature 2019;575:512-518.

[10] **Aran D, Looney AP, Liu L,** Wu E, Fong V, Hsu A, et al. Reference-based analysis of lung single-cell sequencing reveals a transitional profibrotic macrophage. Nat Immunol 2019;20:163-172.

[11] FastQC. 2015 Jun [cited; Available from: https://www.bioinformatics.babraham.ac.uk/projects/fastqc/

[12] **Hao Y, Hao S,** Andersen-Nissen E, Mauck WM, 3rd, Zheng S, Butler A, et al. Integrated analysis of multimodal single-cell data. Cell 2021;184:3573-3587.e3529.

[13] Korsunsky I, Millard N, Fan J, Slowikowski K, Zhang F, Wei K, et al. Fast, sensitive and accurate integration of single-cell data with Harmony. Nat Methods 2019;16:1289-1296.

[14] mm10 murine reference genome downloaded from Ensembl (2018-09-28). [cited; Available from: ftp://ftp.ensembl.org/pub/release-93/fasta/mus_musculus/dna/Mus_musculus.GRCm38.dna_sm.primary_assembly.fa.gz

[15] Dobin A, Davis CA, Schlesinger F, Drenkow J, Zaleski C, Jha S, et al. STAR: ultrafast universal RNA-seq aligner. Bioinformatics 2013;29:15-21.

[16] Love MI, Huber W, Anders S. Moderated estimation of fold change and dispersion for RNA-seq data with DESeq2. Genome Biol 2014;15:550.

[17] **Mootha VK, Lindgren CM,** Eriksson KF, Subramanian A, Sihag S, Lehar J, et al. PGC-1alpha-responsive genes involved in oxidative phosphorylation are coordinately downregulated in human diabetes. Nat Genet 2003;34:267-273.

[18] **Subramanian A, Tamayo P,** Mootha VK, Mukherjee S, Ebert BL, Gillette MA, et al. Gene set enrichment analysis: a knowledge-based approach for interpreting genome-wide expression profiles. Proc Natl Acad Sci U S A 2005;102:15545-15550.

[19] Ucero AC, Bakiri L, Roediger B, Suzuki M, Jimenez M, Mandal P, et al. Fra-2-expressing macrophages promote lung fibrosis in mice. J Clin Invest 2019;129:3293-3309.

[20] Sterling RK, Lissen E, Clumeck N, Sola R, Correa MC, Montaner J, et al. Development of a simple noninvasive index to predict significant fibrosis in patients with HIV/HCV coinfection. Hepatology 2006;43:1317-1325.